DOI 10.1007/s10517-015-2781-4
Bulletin of Experimental Biology and Medicine, Vol. 158, No. 4, February, 2015

PHARMACOLOGY AND TOXICOLOGY

Analysis of Toxicity Biomarkers of Fullerene C_{60} Nanoparticles by Confocal Fluorescent Microscopy

V. A. Shipelin, T. A. Smirnova, I. V. Gmoshinskii, and V. A. Tutelyan

Translated from *Byulleten' Eksperimental'noi Biologii i Meditsiny*, Vol. 158, No. 10, pp. 440-447, October 2014
Original article submitted June 4, 2013

The methods of laser confocal microscopy were employed to study the changes in rat target organs (iliac mucosa and liver) provoked by peroral administration of dispersion of nanosized (31 nm) multimolecular fullerene C_{60} particles in doses of 0.1, 1.0, and 10 mg/kg body weight over 92 days. The micropreparations were selectively stained with fluorescent dyes to mark the cell nuclei (DAPI), actin microfilaments (fluorescently labeled phalloidin), and the membrane proteins CD106, CD31, and claudins in tight junctions (fluorescently labeled monoclonal antibodies). In rats treated with fullerene in the examined doses, the iliac mucosa demonstrated normal morphology of the villi. There were no signs of inflammation and no alterations in the actin filaments of cytoskeleton and in enterocytic tight junctions. The count of $CD106^+$ and $CD31^+$ cells did not change. The highest examined doses of fullerene (1 and 10 mg/kg body weight) increased population and modified distribution of hepatic $CD106^+$ cells. They also resulted in accumulation of cytoplasmic granules presumably identified as Kupffer macrophages without any signs of visible inflammation or necrotic areas. This phenomenon can reflect the early stages of toxic reaction being a sensitive bioindicator of the damage produced by administered fullerene C_{60} in the hepatic tissue.

Key Words: *fullerene; toxicity; ileum; liver; confocal microscopy*

Assessment of the risk for human health resulted from appearance of nanomaterials and the progress of nanotechnologies needs the development of adequate defensive strategy based on the early detection of molecular and cellular markers of the toxic action of these materials [2]. To this end, one can employ the confocal fluorescence microscopy (CFM), a highly informative tool to detect the changes in expression of various proteins in the cells and subcellular structures in the target organs provoked by the action of the nanomaterials on the liver, kidneys, and iliac mucosa [7,9]. In contrast to routine immunohistochemical methods, an important advantage of CFM is the ease of the combined application of several fluorescent probes in the same preparation, which reveals mutual disposition of the examined agents in the specimen.

One of the most promising nanomaterials is fullerene C_{60} with its expected broad use in technology, medicine, and food industry [3]. However, the reliable conclusions on the safe use of fullerene and its analogs in the industrial products that affect human health should be based on the detailed study of all possible facets of their toxic action such as abnormal expression of functionally important proteins in the target organs.

This work was designed to study the effect of fullerene C_{60} dispersion in the doses ranging from 0.1

State Research Institute of Nutrition, Moscow, Russia. ***Address for correspondence:*** gmosh@ion.ru. I. V. Gmoshinskii

to 10 mg/kg body weight on iliac mucosa and liver exerted by its intragastric administration for 92 days.

MATERIALS AND METHODS

The study used fullerene C_{60} (Fullerene-Center) which contained no less than 99.8% basic substance according to reversed-phase chromatography (RPC) data. Prior to administration, the preparation was carefully ground in a mortar. Then a "carrier" was added (2% food starch and 0.5% Tween-80 in deionized water). The ingredients were mixed in a vortex at 3000 rpm for 10 min, thereupon the suspension was sonicated for 3 min at 44 kHz and 2 W/cm^3. Acoustic spectrometry [6] of fullerene dispersion showed that the fullerene molecules aggregated in complexes with bimodal size distribution, the maxima being 31 nm (75% particles by mass) and 660 nm (25%). These data were obtained by Dr. A. A. Loshkarev in ROSNANO Metrological Center.

The experiments were carried out on male Wistar rats (n=24) weighing 100±5 g. The rats were kept in polycarbonate transparent cages (3 animals in each) at 23-25°C with a 12-h day-night cycle. They were maintained on balanced semisynthetic casein diet [14] with water and food *ad libitum*. The rats were randomized into 4 groups of 6 animals. During entire term of experiments (92 days), the group 1 (control) rats were daily administered with intragastric "carrier" solution. The experimental groups 2-4 similarly received fullerene C_{60} dispersed in carrier solution in the doses of 0.1, 1.0, and 10 mg/kg body weight, respectively. In each case, the volume of introduced solution was 1 cm^3/100 g body weight. The rats were sacrificed on day 93 by bleeding under deep ether narcosis, thereafter the liver and ileum were immediately fixed in 10% formalin in PBS (pH 7.4).

The tissue specimens were dehydrated by passing through a series of increasing ethanol concentrations, the mixtures of alcohol and xylene, and pure xylene; thereupon they were embedded in paraffin blocks and mounted in an EC 350 (Microm) apparatus. The thin (5-7 micron) sections were prepared with a Leica RM 2235 microtome, mounted on the slides, and warmed for 10-15 min at 58°C to fix the specimens on the glass. They were deparaffinized by washing two times in xylene and then by passing through 95, 80, and 70% ethanol concentrations, and finally by washing two times in deionized water. The tissue in sections was permeabilized with proteinase K (Sigma, 0.6 U/cm^3 in 0.2 M Tris-HCl buffer) supplemented with 0.05% (weight ratio) Tween-20, thereupon it was stained with specific fluorescent dyes. The following fluorescent labels were employed: DAPI (Invitrogen), phalloidin conjugated with CF568 fluorochrome (Biotium Inc.), antibodies against claudin-1 and the secondary antibodies conjugated with DyLight 488 fluorochrome, antibodies against CD106 (VCAM-1) conjugated with Alexa Fluor 488 fluorochrome, and *4*) antibodies against CD31 labeled with Alexa Fluor 647 (all labels from BioLegend).

The micropreparations were stained with fluorochromes in water media according to the product guide of the fluorescent labels. After staining, the specimens were placed under cover slips with a non-fluorescent medium Mowiol and sealed along the perimeter with a nail-polish to prevent drying.

The specimens were examined under an LSM 710 confocal fluorescence microscope (Carl Zeiss). After mounting on the slides, some ileum specimens were stained with hematoxylin and eosin according to routine method [1] and examined in transmitted light under an Axiolmager ZI microscope (Carl Zeiss) equipped with a color camera.

RESULTS

Figure 1 shows sections of the ileum and liver of control rats, which were stained with DAPI labeling cell nuclei [10] and with antibodies against claudin-1 and phalloidin.

The orange-red fluorescence at λ_{ex}=562 nm and λ_{em}=583 nm revealed binding of phalloidin to F-actin, which made it possible to localize the clusters of actin filaments in the cytoskeleton [8]. Antibodies raised against claudin-1 (green fluorescence) marked this protein, which blocks the paracellular permeability in intercellular tight junctions [15]. While claudin-1 was localized exclusively in tight junctions which occluded the barrier between enterocytes, the most of actin filaments of cytoskeleton were distributed homogeneously across the cytoplasm of enterocytes with the signs of striated staining in the brush border region (Fig. 1, *a*).

In the liver, antibodies against claudin-1 revealed tight junctions between the hepatocytes, which shaped and delimited the bile ducts (Fig. 1, *b*, *c*). Presumably, the brighter phalloidin luminescence regions revealed few hepatic resident macrophages (Kupffer cells) in contrast to prevailing hepatocytes whose luminescence was less intensive (Fig. 1, *a*, *b*).

Another way to process the micropreparations included staining with DAPI and antibodies raised against CD106 and CD31 (green and red fluorescence, respectively). Since emission spectra of the labeled antibodies against CD106 and claudin partially overlapped, these indicators were not used in the same preparation.

In the ileum of control rats, antibodies against CD106 did not stain the preparation (Fig. 1, *d-f*) with rare exceptions of the vessels in ileac wall (Fig. 1, *d*).

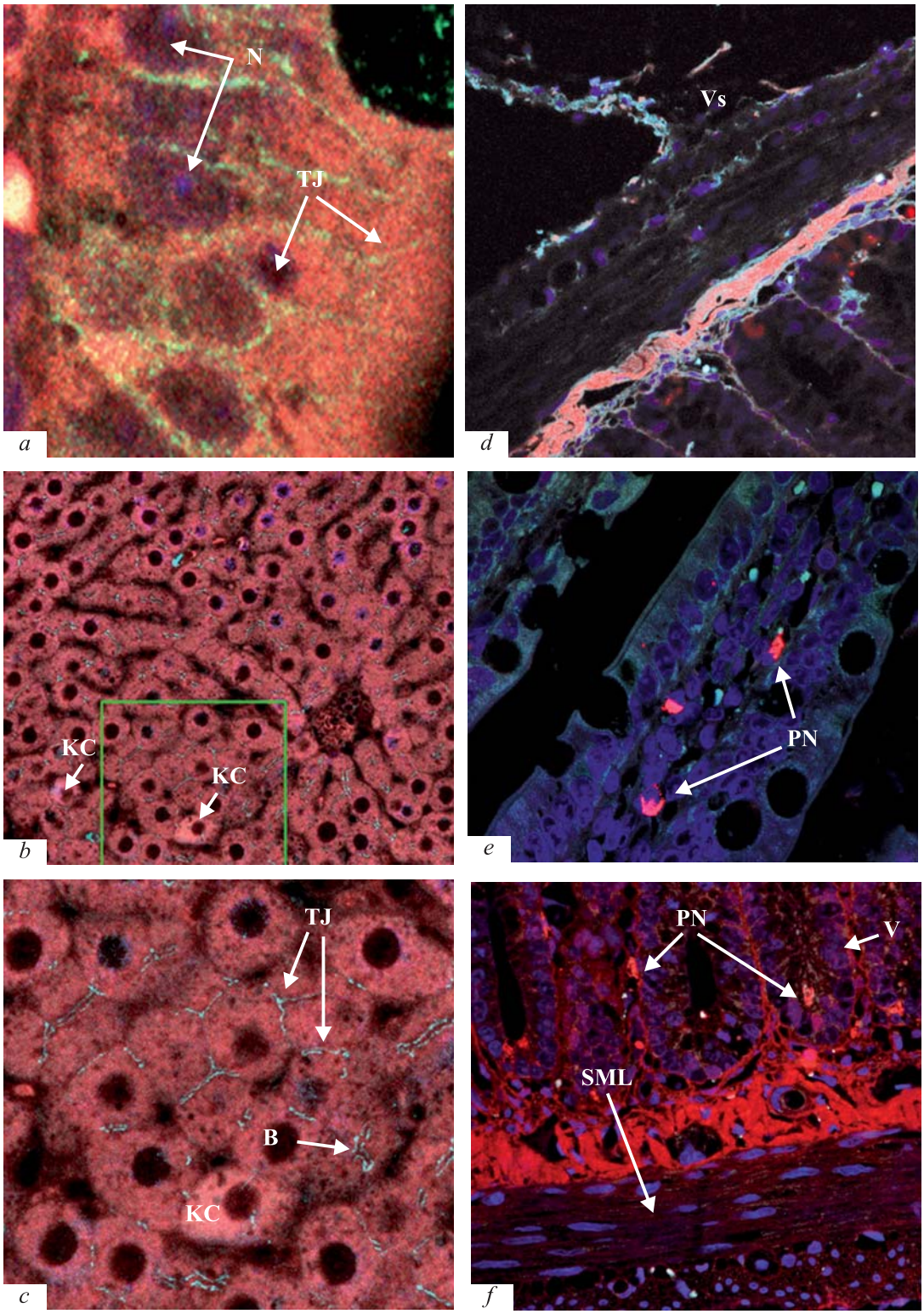

Fig. 1. CFM of ileac (*a*, *d-f*) and hepatic (*b*, *c*) sections of control rat: ×400 (*a*, *d-f*); ×1000 (*b*, *c*). *a-c*: Staining with DAPI (blue), phalloidin (red), and antibodies against claudin (azure); *d-f*: DAPI, antibodies against CD31 (red) and CD106 (azure). N, nuclei; TJ, tight junctions; B, bile ducts; V, villus; SML, smooth muscle layer; Vs, vessel; KC, Kupffer cells (resident hepatic macrophages); PN, presumable neutrophils: CD31-expressing granulated fluorescent cells.

In contrast, antibodies against CDE31 stained the junctions between endotheliocytes (Fig. 1, *f*), the smooth muscle cells in the wall of major vessels, and the granular cells of irregular shape (presumably neutro-

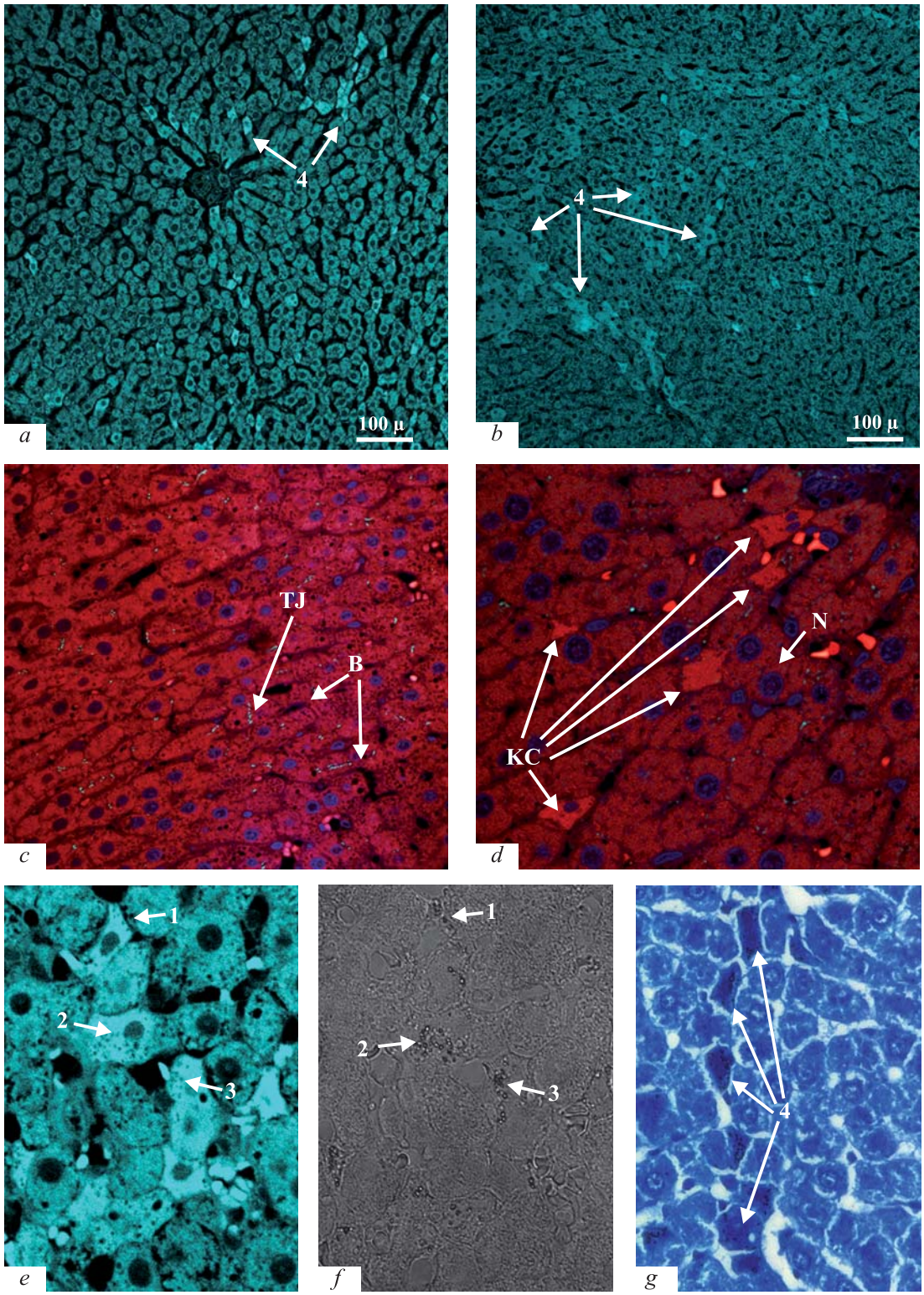

Fig. 2. CFM of hepatic section of group 1 (*a*) and 4 (*b-g*) rats obtained with various staining methods: *a*, *b*, *e*: staining with antibodies against CD106; *c*, *d*: with DAPI, phalloidin, and antibodies against claudin; *f*) the fragment of specimen shown in (*b*) viewed under differential interference contrast in transmitted light; *g*) staining with hematoxylin and eosin. ×400 (*a*, *b*), ×1000 (*c-f*). N, nuclei; TJ, tight junctions; KC, Kupffer cells (presumably); B, bile ducts; *1-4*) $CD106^+$ cells morphologically resembling Kupffer macrophages.

phils) in the region of *lamina propria* of intestinal villi (Fig. 1, *e*, *f*). These cells were mostly located near the crypts, albeit they were also observed in the connective tissue across the entire length of a villus.

TABLE 1. Population of CD31$^+$ Cells in the Ileum of Control and Experimental Rats (*M*±*m*)

Group	Fullerene dose (mg/kg)	Number of cells in a section per 1 mm^2
1 (control; *n*=6)	–	316±126
2 (*n*=3)	0.1	275±66
3 (*n*=3)	1	220±117
4 (*n*=3)	10	156±35*

Note. *p=0.1 in comparison with the control (Student's t test)

Staining of hepatic sections of control rats with antibodies against CD106 (Fig. 2, *a*) revealed enhanced fluorescence in the cytoplasm of small fraction of the hepatic cells. Predominantly, such cells were observed in small numbers in the central area of the lobes, where they were located in the first row near the central veins and major vessels. As a rule, they did not form the clusters and preferred the individual layout. Most of the cells with enhanced luminescence were those with elongated or irregular nucleus, and they were morphologically similar to Kupffer cells.

The morphological presentations of the liver and ileum in group 1 (control) rats and in group 2 experimental rats were virtually identical.

The ileac images obtained in group 3 and 4 rats are shown in Figure 3. In all preparations, antibodies against claudin-1 stained tight junctions between the intestinal epitheliocytes (Fig. 3, *a*, *b*) and revealed no differences in distribution or staining intensity between the rats in control (Fig. 1, *c*) and experimental (Fig. 3, *a*, *b*) groups, which attests to the absence of any alterations in the state of tight junctions of enterocytes under the action of nano- and microparticles of fullerene C_{60}. Staining with phalloidin to label the actin microfilaments in the cells revealed their distribution in enterocytic cytoplasm and in myocytes of the intestinal muscular coat, which corresponded to the norm. This fact attests to the absence of pronounced effects of fullerene on cytoskeleton of intestinal epitheliocytes.

As a rule, antibodies against CD106 did not reveal this protein in group 3 and 4 rats. Similar to the control group, antibodies against CD31 detected expression of this antigen in the cells of irregular shape with pronounced granularity (Fig. 3, *c*-*e*) and located in the connective tissue of intestinal villi and wall (Fig. 3, *f*, *g*). The semi-quantitative analysis of the content of these cells (Table 1) revealed only a decreasing trend of their number in group 4 rats in comparison with the control ones. Morphologically, CD31$^+$ cells in the ileum mucosa resembled neutrophils.

Combined staining with DAPI, phalloidin, and antibodies against claudin-1 revealed no changes in distribution of claudin-1 in the liver of group 3 and 4 rats (Fig. 2, *c*, *d*), which evidences that integrity of the intercellular contacts in the bile ducts was not disturbed. At the same time, the liver of these rats demonstrated an increased population of the cells with enhanced content of actin, as well as the cells with elongated or irregular nucleus, which were presumably the resident hepatic macrophages (Kupffer cells).

In control and experimental rats, staining of hepatic sections with antibodies against CD106 protein revealed the cells with enhanced cytoplasmic luminescence (Fig. 2, *b*, *e*). The share of these cells increased with fullerene dose and attained maximum in groups 3 and 4 rats. The total number of cells with enhanced fluorescence also changed (Table 2).

The clusters of CD106$^+$ cells near the central veins were massive in groups 3 and 4, where the cells were frequently arranged in several rows near these vessels (Fig. 2, *b*). In other regions, CD106$^+$ cells were scattered individually or in small clusters of 2-5 cells. Simultaneous examination of the specimens with CFM and differential interference contrast in transmitted light revealed the contrast granules in almost all such cells (Fig. 2, *f*). The presence of the cells with granules in the hepatic micropreparations of group 3 and 4 rats was corroborated under light microscope in preparations stained with hematoxylin and eosin (Fig. 2, *g*).

When interpreting the data obtained in this study, one should take into consideration that CD106 (VCAM-1) is the protein from immunoglobulin superfamily involved in adhesion of leukocytes with endotheliocytes,

TABLE 2. Population of CD31$^+$ Cells in Hepatic Parenchyma of Control and Experimental Rats

Group	Fullerene dose (mg/kg)	Analyzed section area, mm^2	Total number of cells	Number of cells per 1 mm^2 section
1 (control)	–	22.5	878	39
2	0.1	4.0	206	51
3	1	5.5	802	146
4	10	4.0	517	130

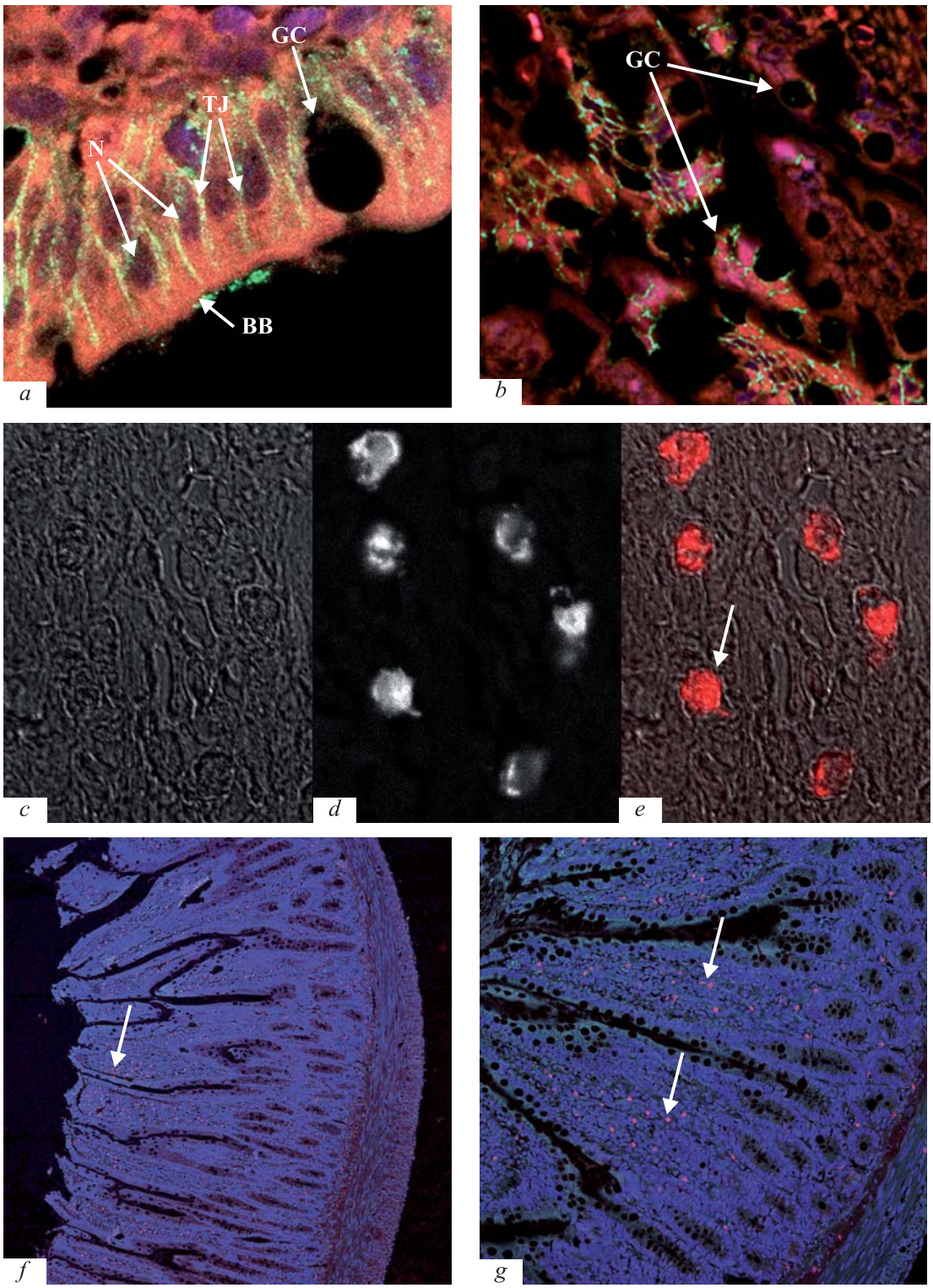

Fig. 3. Ileac wall of group 3 (*a*, axial section) and group 4 (*b*, lateral section) rats. CFM of the sections stained with DAPI, phalloidin, and antibodies against claudin. *c-e*: $CD31^+$ cells in ileac wall viewed under differential interference contrast in transmitted light, CFM, and superposition of these images, respectively. *f*, *g*: CFM of ileac wall section of groups 3 and 4 rats, respectively, stained with DAPI as well as antibodies against CD31 and CD106. ×1000 (*a-e*), ×400 (*f*, *g*). N, nuclei; TJ, tight junctions; GC, goblet cell; BB, brush border.

in transmission of cellular signals, and in mediation during adhesion of lymphocytes, monocytes, eosinophils, and basophils to vascular endotheliocytes during the subacute stage of inflammation [4]. Usually this protein is expressed in the walls of large and small blood vessels after stimulation of the endotheliocytes

with cytokines, so it can be viewed as a marker of activation of endothelium by cytokines [5,11].

CD31 (PECAM-1) is a membrane glycoprotein from immunoglobulin superfamily, which belongs to the class of the cell adhesion molecules and to the subgroup of proteins with inhibitory ITIM cite [13]. It is the universal marker of normal endothelium [12]. In small numbers, this glycoprotein is observed in circulating platelets, monocytes, neutrophils, and in some populations of T lymphocytes. CD31 is involved in transendothelial migration of leukocytes during acute stage of inflammation, in angiogenesis and in activation of integrins. Moreover, CD31 is a membrane mechanoreceptor, which triggers a cascade of reactions in endotheliocytes in response to shear stress produced by blood flow.

The present CFM morphological study of presumable fullerene target organs revealed no alterations in iliac mucosa for 3 month when fullerene was daily administered in the doses below 10 mg/kg. During this period, the normal morphology of the villi did not change; there were no signs of inflammation or expansion of the neutrophil population in the tissue. The intercellular contacts and the actin microfilament system in enterocytes were not disturbed. However, the greatest examined dose of fullerene (10 mg/kg) increased population and changed distribution of $CD106^+$ cells accompanied by accumulation of the granules in cytoplasm (Fig. 2, *b-d*; Fig. 3, *c-e*), which probably attests to activation of the cells (presumably identified as Kupffer macrophages) in the absence of the overt signs of inflammation or necrotic areas. This effect can evidence the development of the early stages of toxic reaction being a sensitive bioindicator of the damaging action of fullerene C_{60} in the hepatic tissue.

REFERENCES

1. *Microscopy Methods: A Textbook* [in Russian], Eds. D. L. Sarkisov and Yu. L. Perov, Moscow (1996).
2. G. G. Onishchenko, V. A. Tutelyan, I. V. Gmoshinskii, and S. A. Khotimchenko, *Gig. Sanit*., No. 1, 4-11 (2013)
3. L. B. Piotrovskii and O. I. Kiselev, *Fullerenes in Biology: Go Marching in Nanomedicine* [in Russian], St. Petersburg (2006).
4. J. L. Baron, E.P. Reich, I. Visintin, and C. A. Janeway, *J. Clin. Invest*., **93**, No. 4, 1700-1708 (1994).
5. R. A. Carter and I. P. Wicks, *Arthritis Rheum*., **44**, No. 5, 985-994 (2001).
6. A. S. Dukhin and P. J. Goetz, *Ultrasound for Characterizing Colloids – Particle Sizing, Zeta Potential, Rheology*, Eds. D. Moebius and R. Miller, Amsterdam (2002).
7. E. Frohlich and E. Roblegg, *Toxicology*, **291**, Nos. 1-3, 10-17 (2012).
8. Z. J. Huang, R. P. Haugland, W. M. You, and R. P. Haugland, *Anal. Biochem*., **200**, No. 1, 199-204 (1992).
9. P. Jani, G. W. Halbert, J. Langridge, and A. T. Florence, *J. Pharm. Pharmacol*., **42**, No. 12, 821-826 (1990).
10. J. Kapuscinski, *Biotech. Histochem*., **70**, No. 5, 220-233 (1995).
11. P. A. Koni, S. K. Joshi, U. A. Temann, *et al*., *J. Exp. Med*., **193**, No. 6, 741-754 (2001).
12. J. L. McQualter, N. Brouard, B. Williams, *et al*., *Stem Cells*, **27**, No. 3, 623-633 (2009).
13. P. J. Newman, *J. Clin. Invest*., **99**, No. 1, 3-8 (1997).
14. P. G. Reeves, F. H. Nielsen, and G. C. Fahey Jr., *J. Nutr.*, **123**, No. 11, 1939-1951 (1993).
15. J. R. Turner, *Am. J. Pathol*., **169**, No. 6, 1901-1909 (2006).